



# Open Research Online

---

The Open University's repository of research publications and other research outputs

## Negative ion formation in potassium–nitromethane collisions

### Journal Item

How to cite:

Antunes, R.; Almeida, D.; Martins, G.; Mason, N. J.; Garcia, G.; Maneira, M. J. P.; Nunes, Y. and Limão-Vieira, P. (2010). Negative ion formation in potassium–nitromethane collisions. *Physical Chemistry Chemical Physics*, 12(39) pp. 12513–12519.

For guidance on citations see [FAQs](#).

© 2010 the Owner Societies

Version: Version of Record

Link(s) to article on publisher's website:  
<http://dx.doi.org/doi:10.1039/c004467a>

---

Copyright and Moral Rights for the articles on this site are retained by the individual authors and/or other copyright owners. For more information on Open Research Online's data [policy](#) on reuse of materials please consult the policies page.

---

[oro.open.ac.uk](http://oro.open.ac.uk)

# Negative ion formation in potassium–nitromethane collisions

R. Antunes,<sup>a</sup> D. Almeida,<sup>a</sup> G. Martins,<sup>a</sup> N. J. Mason,<sup>b</sup> G. Garcia,<sup>cd</sup>  
M. J. P. Maneira,<sup>a</sup> Y. Nunes<sup>a</sup> and P. Limão-Vieira<sup>\*ab</sup>

Received 18th March 2010, Accepted 29th June 2010

DOI: 10.1039/c004467a

Ion-pair formation in gaseous nitromethane ( $\text{CH}_3\text{NO}_2$ ) induced by electron transfer has been studied by investigating the products of collisions between fast potassium atoms and nitromethane molecules using a crossed molecular-beam technique. The negative ions formed in such collisions were analysed using time-of-flight mass spectroscopy. The six most dominant product anions are  $\text{NO}_2^-$ ,  $\text{O}^-$ ,  $\text{CH}_3\text{NO}_2^-$ ,  $\text{OH}^-$ ,  $\text{CH}_2\text{NO}_2^-$  and  $\text{CNO}^-$ . By using nitromethane- $\text{d}_3$  ( $\text{CD}_3\text{NO}_2$ ), we found that previous mass 17 amu assignment to  $\text{O}^-$  delayed fragment, is in the present experiment may be unambiguously assigned to  $\text{OH}^-$ . The formation of  $\text{CH}_2\text{NO}_2^-$  may be explained in terms of dissociative electron attachment to highly vibrationally excited molecules.

## 1. Introduction

In this paper we report the results of a new experimental investigation of negative ion formation in potassium–nitromethane collisions. Ion formation is explored at different collision energies and deuterated nitromethane is used to identify some of the fragments that were ill-defined in previous experiments.

Nitromethane,  $\text{CH}_3\text{NO}_2$ , has been studied extensively both experimentally<sup>1–13</sup> and theoretically<sup>14–17</sup> because it is; (1) an important compound in the chemistry of the Earth's troposphere and stratosphere; (2) a nitro–organic molecule used in the production of explosives and propellants; (3) a prototypical molecule which can be used as a benchmark system for high-level computational modelling of molecular energetics and structural properties and (4) it is a polar molecule with a considerable static dipole moment allowing dipole-bound anion states to be formed by the capture of an extra electron.

Stockdale *et al.*<sup>6</sup> have investigated by electron impact and collisions with atoms in excited Rydberg states (see more recently Suess *et al.*<sup>9</sup>), the production of negative ions from nitromethane; parent ion formation through charge transfer reactions of Rydberg states was demonstrated by the acceptor molecule only *via* a three-body mechanism. Previous work on ion-pair formation in collisions of potassium atoms with nitromethane molecules have been reported including double-differential cross sections, obtained as a function of the scattered angle and the post-collision energy.<sup>12</sup> However, in this study only relative total partial cross section measurements were obtained and only three negative ions,  $\text{O}^-$ ,  $\text{NO}_2^-$  and  $\text{CH}_3\text{NO}_2^-$  were detected. Steric asymmetry studies in electron

transfer from potassium atoms to oriented nitromethane molecules have been performed by Brooks and co-workers,<sup>13</sup> showing no steric evidence for methyl-end attack favouring the participation of a dipole-bound state in the formation of  $\text{CH}_3\text{NO}_2^-$  near the threshold.

Compton and co-workers<sup>5</sup> have also studied the collisional ionisation mechanism between alkali atoms (Na, K, Cs) and some methane derivatives (including  $\text{CH}_3\text{NO}_2$ ), from threshold up to  $\sim 40$  eV and from the energy thresholds of specific ion-pair production reactions derived electron affinity values for the stable negative ions. Liu *et al.*<sup>10</sup> have explored charge transfer in collisions between dipole-bound  $\text{CH}_3\text{CN}^-$  negative ions and  $\text{CH}_3\text{NO}_2$  in Penning ion trap experiments.

The spectroscopy and dissociation dynamics of nitromethane and its anionic states have been investigated using optical and electron scattering methods by Walker and Palmer.<sup>3</sup> Modelli and Venuti<sup>4</sup> have measured the resonance energies of  $\text{CH}_3\text{NO}_2$  by means of electron transmission spectroscopy and explored dissociative electron attachment over the electron energy range from 0–6 eV. Dissociative electron attachment (DEA) to nitromethane has been investigated in the electron energy range 0–10 eV by Sailer *et al.*<sup>2</sup> using a high energy resolution (140 meV) electron beam, with 7 fragment anions detected. Recently, Alizadeh *et al.*<sup>1</sup> have revisited these DEA measurements making use of a high mass-resolution sector field instrument. Anion efficiency curves for 16 negatively charged fragments were obtained in the electron energy range from 0 to 16 eV, with an energy resolution of  $\sim 1$  eV.

Dipole- and valence-bound anion states of nitromethane have been reported using negative ion photoelectron spectroscopy (see also ref. 11 for photoelectron imaging) and Rydberg charge exchange and field detachment techniques<sup>7</sup> of both bare and argon-solvated anions;<sup>8</sup> these studies have shown that the dipole-bound and valence forms of nitromethane are interconnected with no appreciable potential barrier ( $\sim 12$  meV) relative to zero-point vibrational motion. Adamowicz<sup>14</sup> performed *ab initio* coupled cluster studies of the dipole-bound anionic states of nitromethane and obtained an electron affinity of  $\sim 3$  meV, much lower than the experimental value obtained by Compton *et al.*<sup>7</sup>

<sup>a</sup> Laboratório de Colisões Atómicas e Moleculares, CEFITEC, Departamento de Física, FCT, Universidade Nova de Lisboa, 2829-516 Caparica, Portugal. E-mail: plimaovieira@fct.unl.pt; Fax: +351-21 294 85 49; Tel: +351-21 294 85 76

<sup>b</sup> Centre of Earth, Planetary, Space and Astronomy Research, Department of Physics and Astronomy, The Open University, Walton Hall, Milton Keynes, UK MK7 6AA

<sup>c</sup> Instituto de Física Fundamental, Consejo Superior de Investigaciones Científicas, Serrano 113-bis, 28006 Madrid, Spain

<sup>d</sup> Departamento de Física de los Materiales, UNED, Senda del Rey 9, 28040 Madrid, Spain

Theoretical studies on the coupling between valence- and dipole-bound states of nitromethane<sup>15,16</sup> have shown that, upon electron capture, the diffuse dipole-bound state accommodates the electron's kinetic energy within the molecule's vibrational degrees of freedom *via* a vibrational Feshbach resonance. Due to non-adiabatic coupling with the molecule's valence states, the extra electron may be transferred into a valence orbital competing with a process that is in competition with autodetachment. However, owing to the electron affinities of the valence states, the dissociation channels that become available and the intermolecular energy redistributions that can occur, long-lived anions can be formed that compete with anionic fragments formed by dissociation.

## 2. Experimental procedure

The present time-of-flight (TOF) mass spectra of the anions produced in K-nitromethane- $\text{h}_3$  and nitromethane- $\text{d}_3$  interactions were measured in a crossed molecular beam set-up.<sup>18</sup> Briefly, a nitromethane beam crossed a primary beam of fast neutral potassium (K) atoms derived from a charge-exchange source.  $\text{K}^+$  ions were produced in a potassium ion source and

accelerated, in the present experiments from 30–100 eV, through an oven where they charge exchange resonantly with neutral potassium to produce a beam of fast (hyperthermal) atoms. Residual ions from the primary  $\text{K}^+$  beam are removed by electrostatic deflecting plates placed outside the oven.

The hyperthermal alkali beam enters a high vacuum chamber where its intensity is monitored by an iridium surface ionisation detector of the Langmuir–Taylor type. This detector samples the beam intensity but does not interfere with the beam passing into the collision region. It operates in a temperature regime that only allows detection of the fast beam. An effusive beam of nitromethane is introduced into a 1 mm diameter source into the interaction region where it intersects the neutral hyperthermal potassium beam. The typical base pressure in the collision chamber was  $4 \times 10^{-5}$  Pa and upon gas admission increased to a pressure of  $6 \times 10^{-4}$ – $2 \times 10^{-3}$  Pa.

The collision volume is located in the middle of two parallel plates placed 1.2 cm apart. Negative ions formed in the interaction region are removed in a direction normal to the plane of the two crossing beams by a  $\sim 250$  V  $\text{cm}^{-1}$  pulsed electrostatic field and TOF mass analysed; the hyperthermal neutral atoms pulse width is 2  $\mu\text{s}$  with a frequency of 100 eV - 22 kHz (70 eV, 30 eV - 11 kHz).<sup>18</sup> The spectra in Fig. 1 and 2 showing the recorded anionic signals are obtained by subtracting the background signal from the sample signal.

The anion mass spectra show a peculiar feature in the shape of the  $\text{H}^-$  TOF structures due to a shoulder in the peaks' right side (Fig. 1). This contribution is an artefact from the potassium hyperthermal neutral atoms ( $\text{K}^\circ$ ) pulsed signal and is most likely related to the rate of creation of negative ions while the  $\text{K}^\circ$  beam is still in the interaction region. The width of the shoulder has been shown not to interfere with the neighbouring anions (see discussion below).

### Nitromethane samples

The liquid samples of nitromethane- $\text{h}_3$  and - $\text{d}_3$  were purchased from Sigma-Aldrich with a minimum purity of  $\geq 96\%$  and  $99\%$ , respectively. The nitromethane- $\text{h}_3$  compound has been purified. All samples were degassed by a repeated freeze–pump–thaw cycle before admission to the collision chamber.

## 3. Results and discussion

In contrast to the previous TOF mass spectrum reported by ref. 12, we were able to detect nine new anions (Table 1), all peaks being observed with better resolution than before.<sup>12</sup> Electron transfer from potassium atoms to nitromethane molecules produces the parent ion  $\text{CH}_3\text{NO}_2^-$ , the dehydrogenated closed-shell anion  $[\text{CH}_2\text{NO}_2\text{--H}]^-$ ,  $\text{NO}_2^-$ ,  $\text{CNO}^-$ ,  $\text{OH}^-$ ,  $\text{O}^-$  and some other minor intensity fragment ions.

Fig. 1(a) shows the TOF mass spectra of the anions formed in the collision of  $\text{K} + \text{CH}_3\text{NO}_2$ , recorded at an incident potassium energy of 30, 70 and 100 eV, normalised to the most intense peak,  $\text{NO}_2^-$ , whereas Fig. 1(b) shows an expanded view at 100 eV. From the TOF mass spectra we observe that the two major anionic fragments are  $\text{NO}_2^-$  and  $\text{O}^-$ , anions with masses 45 and 17 have less than 10% of the total yield. At 30 eV the  $\text{O}^-$  intensity is about 15% of the  $\text{NO}_2^-$  peak, while at 100 eV  $\text{O}^-$  is about one-third of the

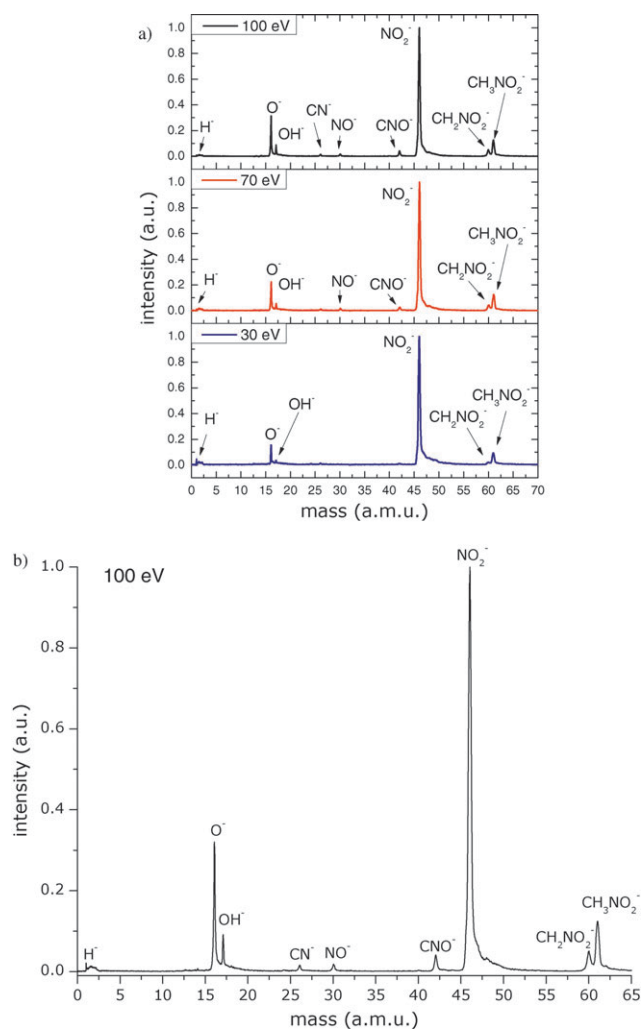


**Fig. 1** Negative ion time-of-flight mass spectra of  $\text{K} + \text{CH}_3\text{NO}_2$  at: (a) 100, 70 and 30 eV collision energy; (b) expanded view at 100 eV.

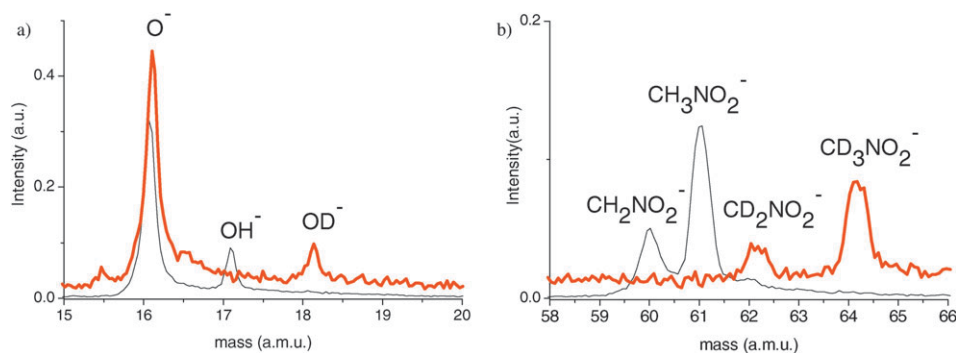


**Fig. 2** Negative ion time-of-flight mass spectrum of  $\text{K} + \text{CH}_3\text{NO}_2$  and  $\text{K} + \text{CD}_3\text{NO}_2$  at 100 eV collision energy: (a)  $\text{O}^-$ ,  $\text{OH}^-$  and  $\text{OD}^-$  formation; (b)  $\text{CH}_2\text{NO}_2^-$ ,  $\text{CH}_3\text{NO}_2^-$ ,  $\text{CD}_2\text{NO}_2^-$  and  $\text{CD}_3\text{NO}_2^-$  formation.

dominant  $\text{NO}_2^-$  structure. This strongly indicates that the energy of the resonant state resulting in  $\text{O}^-$  is higher than the state yielding  $\text{NO}_2^-$  and is consistent with the electron attachment spectroscopy results of Alizadeh *et al.*<sup>1</sup> and Sailer *et al.*<sup>2</sup> While  $\text{NO}_2^-$  and  $\text{O}^-$  may result from single bond cleavage in the decomposition of the transient negative ion, the formation of  $\text{CNO}^-$ ,  $\text{OH}^-$  (and  $\text{CN}^-$ ) may result from more complex reactions involving multi-bond cleavage and internal energy rearrangement. This will be discussed in detail below.

In atom–molecule collisions leading to the formation of ion-pairs, the target (electron acceptor) molecule is expected to react easily if it has anionic states which match the instantaneous kinetic energy of the incoming “bound” electron. The anionic states in nitromethane have been found by electron impact<sup>3</sup> to lie at 0.72, 2.4, 4.0, 5.6, 6.1 and 8.6 eV (Table 2), with the exception of the 2.4 eV state which has shown to be non-dissociative. In previous studies of ion-pair formation in collisions between K atoms and  $\text{CH}_3\text{NO}_2$  molecules,<sup>12</sup> both ionic and inelastic channels have been explored; three anionic states have been identified as intermediates for the final anion fragment production, especially a repulsive  $\sigma^*$  state of ( $^2A_1$ ) symmetry and two bound states of  $^2B_1(\pi^*)$  character. A vertical electron affinity of  $-2.16 \pm 0.17$  eV was obtained for the  $^2A_1(\sigma^*)$  and this anionic state decays by both auto-detachment and dissociation into ( $\text{CH}_3 + \text{NO}_2^-$  ( $^1A_1$ )).

We will now discuss the formation mechanisms of each anion observed in the TOF spectra and critically compare them with gas phase DEA measurements and, where practical, with available theoretical calculations.

### 3.1 $\text{CH}_3\text{NO}_2^-$

The parent anion formation  $\text{CH}_3\text{NO}_2^-$  ( $^2B_1$  anion ground state) was observed *via* the attachment of a Rydberg electron and may be formed from the metastable  $(\text{CH}_3\text{NO}_2)^-*$  anion which may subsequently relax to a geometry where auto-detachment channels may be blocked.<sup>6</sup> The  $^2B_1$  anion ground state, which is strongly bound along the C–N coordinate, correlates with an excited ( $^3B_1$ ) state of  $\text{NO}_2^-$ , which lies 2.31 eV above the ground  $^1A_1$  state of  $\text{NO}_2^-$ .<sup>12</sup> Walker and Fluendy’s computations<sup>3</sup> predict for the  $^2B_1$  state an extended NO bond and suggest that, upon low energy electron attachment, a maximum of 0.6 eV is stored in the vibrational symmetric mode of the  $\text{NO}_2$  group. Therefore, this state will be vibrationally excited in either a C–N or N–O stretching mode. Theoretical studies of the structure of the anion indicate substantial change in these bond lengths, where the N–O bond in the anion is increased by  $\sim 0.1$  Å and the tilting of the O–N–O plane changes from approximately zero in the neutral to  $\sim 35^\circ$  in the anion.<sup>16</sup> However, as long as the vibrationally excited anion lies above the ground-state of the neutral, there

**Table 1** Anionic species formed following electron attachment and electron transfer to nitromethane

| M (a.m.u.) | Anionic species            | Ref. 1 | Ref. 2 | Ref. 3 | Ref. 12 | Ref. 19 | This work |
|------------|----------------------------|--------|--------|--------|---------|---------|-----------|
| 1          | $\text{H}^-$               | ✓      | ✗      | ✗      | ✗       | ✗       | ✓         |
| 13         | $\text{CH}^-$              | ✓      | ✓      | ✓      | ✗       | ✓       | ✗         |
| 14         | $\text{CH}_2^-$            | ✓      | ✓      | ✗      | ✗       | ✗       | ✗         |
| 15         | $\text{CH}_3^-$            | ✓      | ✗      | ✗      | ✗       | ✗       | ✗         |
| 16         | $\text{O}^-$               | ✓      | ✓      | ✓      | ✓       | ✓       | ✓         |
| 17         | $\text{OH}^-$              | ✓      | ✓      | ✓      | ✗       | ✓       | ✓         |
| 18         | $^{18}\text{O}^-$          | ✓      | ✗      | ✗      | ✗       | ✗       | ✗         |
| 26         | $\text{CN}^-$              | ✓      | ✓      | ✓      | ✗       | ✓       | ✓         |
| 30         | $\text{NO}^-$              | ✓      | ✓      | ✗      | ✗       | ✓       | ✓         |
| 32         | $\text{H}_2\text{NO}^-$    | ✓      | ✗      | ✗      | ✗       | ✗       | ✗         |
| 42         | $\text{CNO}^-$             | ✓      | ✓      | ✓      | ✗       | ✓       | ✓         |
| 44         | $\text{CH}_2\text{NO}^-$   | ✓      | ✗      | ✗      | ✗       | ✗       | ✗         |
| 46         | $\text{NO}_2^-$            | ✓      | ✓      | ✗      | ✓       | ✓       | ✓         |
| 47         | $^{15}\text{NO}_2^-$       | ✓      | ✗      | ✗      | ✗       | ✗       | ✗         |
| 59         | $\text{CHNO}_2^-$          | ✓      | ✗      | ✗      | ✗       | ✓       | ✗         |
| 60         | $\text{CH}_2\text{NO}_2^-$ | ✓      | ✗      | ✗      | ✗       | ✓       | ✓         |
| 61         | $\text{CH}_3\text{NO}_2^-$ | ✗      | ✗      | ✗      | ✓       | ✗       | ✓         |

**Table 2** Anionic states and major decay products of nitromethane

| -EA <sub>v</sub> /eV [3]/[12] | Anionic states   | Decay products   |  |   |
|-------------------------------|--|--|--|---|
|                               |  | Present work   | Electron impact (ref. 3)   | Alkali beam (ref. 12)   |
| 0.72/-                        | <sup>2</sup> B <sub>1</sub> (π* NO)  | CH <sub>3</sub> NO <sub>2</sub> <sup>-</sup><br>O <sup>-</sup>   | NO <sub>2</sub> <sup>-</sup> (via <sup>2</sup> A <sub>1</sub> )<br>CH <sub>3</sub> NO <sub>2</sub> <sup>vib</sup> + e <sup>-</sup> | CH <sub>3</sub> NO <sub>2</sub> <sup>-</sup><br>O <sup>-</sup>  |
| 2.4/2.16                      | <sup>2</sup> A <sub>1</sub> (σ* CN, σ* CH)   | CH <sub>2</sub> NO <sub>2</sub> <sup>-</sup><br>NO <sub>2</sub> <sup>-</sup><br>CN <sup>-</sup> , CNO <sup>-</sup>   | —<br>CH <sub>3</sub> NO <sub>2</sub> <sup>vib</sup> + e <sup>-</sup><br>—  | NO <sub>2</sub> <sup>-</sup><br>CH <sub>3</sub> NO <sub>2</sub> <sup>vib</sup> + e <sup>-</sup><br>—        |
| 4.0/-                         | <sup>2</sup> B <sub>1</sub><br><sup>2</sup> B <sub>2</sub> (σ* CH <sub>3</sub> )<br><sup>2</sup> A <sub>1</sub> (σ* CN, σ* NO) | CH <sub>3</sub> NO <sub>2</sub> <sup>-</sup> , OH <sup>-</sup><br>NO <sub>2</sub> <sup>-</sup><br>O <sup>-</sup><br>CH <sub>2</sub> NO <sub>2</sub> <sup>-</sup><br>CN <sup>-</sup> , CNO <sup>-</sup> | OH <sup>-</sup> , CN <sup>-</sup> , CNO <sup>-</sup><br>—<br>—<br>—<br>—   | CH <sub>3</sub> NO <sub>2</sub> <sup>-a</sup><br>NO <sub>2</sub> <sup>-a</sup><br>O <sup>-a</sup><br>—<br>— |
| 5.6/-                         | —  | O <sup>-</sup> , OH <sup>-</sup>   | O <sup>-</sup> , OH <sup>-</sup> , CH <sup>-</sup>   | —   |
| 6.1/-                         | —  | O <sup>-</sup>   | O <sup>-</sup>   | —   |
| 8.6/-                         | —  | O <sup>-</sup> , OH <sup>-</sup> , H <sup>-</sup>  | O <sup>-</sup> , OH <sup>-</sup> , CN <sup>-</sup> , CNO <sup>-</sup>  | —   |

<sup>a</sup> Assigned to an excited state of <sup>2</sup>B<sub>1</sub> symmetry.

is strong competition with autodetachment, which has been shown to dominate the vibrationally inelastic channel at low energy losses.<sup>16</sup>

Nitromethane has a dipole moment of 3.46 D, and therefore can support a stable dipole-bound state (DBS) and so, under appropriate conditions, a weakly bound electron (*e.g.*, in a Rydberg state) can be transferred to form a dipole-bound anion which may serve as a “doorway” to valence states.<sup>7</sup> Indeed recent calculations for electron attachment to nitromethane<sup>15</sup> have shown that, on a mass spectrometric timescale, the dipole bound anion serves as an efficient doorway to a valence state, which is quickly populated and may be stabilised by collisions with a third body partner.

Dipole-bound states of CH<sub>3</sub>NO<sub>2</sub> have been reported before<sup>5</sup> and can develop into two states of the same <sup>2</sup>A symmetry (which correlates with <sup>2</sup>A<sub>1</sub> in C<sub>2v</sub> symmetry) when the amplitude of the tilting angle (the deviation of the ONO plane from the vertical line passing through the C–N bond) is particularly large (–20° ≥ θ<sub>tilt</sub> ≥ +20°). Sommerfeld’s theoretical results on the coupling between dipole-bound and valence states,<sup>15</sup> obtained a value of about 30 meV for the non-adiabatic coupling element, H<sub>12</sub>, which is particularly small with respect to the vertical excitation energies of the anionic states (see Table 2). The coupling in nitromethane is therefore considered weak and the description of transitions between dipole-bound and the valence states may be explained as diabatic.

Compton *et al.*<sup>7</sup> studies of the electric field detachment through Xe(*nf*) reactions and laser photodetachment photoelectron spectroscopy to CH<sub>3</sub>NO<sub>2</sub>, yield a value of (0.012 ± 0.003) eV and (0.26 ± 0.08) eV for the dipole-bound and valence adiabatic electron affinities, respectively. However, these field detachment studies have also revealed that dipole-bound states couple with valence states due to partial stabilisation induced by collisions with the Rydberg core. This is consistent with a three-body mechanism where charge transfer reactions of Rydberg states occur, which also applies to the present alkali beam experiment. As the reaction proceeds, the ion geometry with respect to the neutral will bend allowing a stable ion to survive, at least over the detection time window.<sup>7</sup> This is reminiscent of a covalent electron binding mechanism observed in the laser photodetachment experiments,<sup>7</sup> with the

particular attention to the wagging motion of the –NO<sub>2</sub> group (that undergoes significant changes upon binding an extra electron) through a breakdown in the Born–Oppenheimer approximation of the molecular system. It is interesting to note that Compton *et al.*<sup>7</sup> realised that, for a small –NO<sub>2</sub> angular tilting, a small barrier between the dipole- and valence-bound states is formed, so the metastable dipole state lives a long time if it vibrationally couples with the anion ground (valence) state.

Electron attachment to form a transient negative valence anion can occur *via* a nuclear excited Feshbach resonance as well as *via* dipole-supported shape and vibrational Feshbach resonances in the continuum as suggested by Sommerfeld<sup>15</sup> and Gustev and Barlett.<sup>16</sup> The system may then be rationalised in terms of dipole states acting as doorways to the eventual formation of stable valence anions, as long as they exist in the continuum. For the particular case of Rydberg electron transfer experiments, Compton *et al.*<sup>7</sup> considered that the coupling between pure dipole and valence states occurs through breakdown of the Born–Oppenheimer approximation. Moreover, they suggested that the ratio of the time spent in the pure dipole-(D<sup>-</sup>) to valence-state (V<sup>-</sup>) is given by the ratio of the density of states, ρ<sub>D<sup>-</sup></sub>/ρ<sub>V<sup>-</sup></sub>.<sup>7</sup> They found that this ratio is negligible; therefore, they expected the system to spend most of the time in the valence configuration. If the anion is vibrationally excited (hot bands) and this internal energy is not removed by stabilisation with a third body, autodetachment becomes relevant. This is in agreement with discussion on the electron attachment studies by Walker and Fluendy<sup>3</sup> and may also explain the observations of the present experiments, where the intensity of the CH<sub>3</sub>NO<sub>2</sub><sup>-</sup> anion is never the strongest, suggesting that autodetachment competes with dissociation and dictates the intensity of the parent ion formation.

### 3.2 CH<sub>2</sub>NO<sub>2</sub><sup>-</sup>

The dehydrogenated closed shell anion CH<sub>2</sub>NO<sub>2</sub><sup>-</sup> may be formed *via* the following endothermic dissociative electron attachment process:<sup>1</sup>

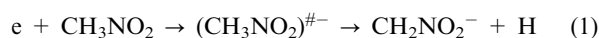




**Table 3** Gas phase standard heats of formation ( $\Delta H_f^\circ$ ) and electron affinities relevant in dissociative electron attachment to nitromethane

| Compound                                      | $\Delta H_f^\circ/\text{kJ mol}^{-1}$ | Electron Affinity/eV   |
|---|---------------------------------------|--|
| CH <sub>3</sub> NO <sub>2</sub>               | -81 ± 1                               | 0.44 ± 0.20 (adiabatic)<br>-0.72 (vertical)<br>0.012 ± 0.003<br>(dipole-bound state) |
| CH <sub>2</sub> NO <sub>2</sub>               |                                       | 2.45 (ref. 1)  |
| NO <sub>2</sub>                               | 33.1                                  | 2.2730 ± 0.0050  |
| CNO   | —                                     | 3.6090 ± 0.0050  |
| CN  | 435.14                                | 3.8620 ± 0.0050  |
| O   | 249.18 ± 0.10                         | 1.461112 ± 0.000044  |
| CH <sub>3</sub>                               | 146 ± 1                               | 0.080 ± 0.030  |
| H   |                                       | 0.75   |
| CH <sub>3</sub> NO <sub>2</sub> <sup>-</sup>  | -100.0 ± 7.9                          | —  |
| NO <sub>2</sub> <sup>-</sup>                  | 82.84                                 | —  |
| O <sup>-</sup>                                | 108.3                                 | —  |
| Bond dissociation energies/eV                 |                                       |  |
| CH <sub>3</sub> -NO <sub>2</sub>              | 2.64                                  |  |
| CH <sub>3</sub> NO-O                          | 4.76                                  |  |
| CH <sub>2</sub> NO <sub>2</sub> -H            | 4.40                                  |  |
| CH <sub>3</sub> -NO <sub>2</sub> <sup>-</sup> | 0.56 ± 0.20                           |  |

with a threshold at 1.95 eV, obtained through the bond energy  $D(\text{CH}_2\text{NO}_2\text{-H}) = 4.40$  eV and the electron affinity  $\text{EA}(\text{CH}_2\text{NO}_2) = 2.45$  eV (Table 3). However, Alizadeh *et al.*<sup>1</sup> reported lower resonant feature leading to  $\text{CH}_2\text{NO}_2^-$  formation at  $\sim 0.5$  eV, which is not energetically allowed. However, as is the case for  $\text{NO}_2^-$  formation (see below), electron attachment can only proceed through vibrationally excited states (hot bands) even though the number density of such "hot" molecules may be low, electron attachment cross sections for excited states are often orders of magnitude higher than those in the ground state. Such behaviour has been previously reported by Illenberger and co-workers for the case of  $\text{CF}_3\text{Cl}$ .<sup>20</sup>

The formation of  $\text{CH}_2\text{NO}_2^-$  and  $\text{CH}_3\text{NO}_2^-$  ions were observed in the proportion of  $\sim 1:3$ , respectively, and were similar for all the three collision energies studied, 30, 70 and 100 eV. Although, it is reasonable to assume that the energy of the resonant states resulting in the nitromethane parent anion and the dehydrogenated closed shell anion  $\text{CH}_2\text{NO}_2^-$  are identical, and the latter cannot be formed through direct electron capture but rather due to the transient  $\text{CH}_3\text{NO}_2^*$  anion, which is in clear agreement with the fact that the parent anion is a precursor for the formation of this anion. The dehydrogenated parent ion formation can actually be seen from an interesting point of view regarding the strong coupling between the dipole bound state and the temporary anion state related to the occupation of valence  $\pi^*$  orbitals, that actually play a significant role in electron capture by nitromethane molecules.

The LUMOs in nitromethane are at approximately 0.72 ( $\pi^*(b_1)$ ), 2.4 ( $\sigma^*(a_1)$ ), 4.0, 5.6, 6.1 and 8.6 eV.<sup>3</sup> As the asymptotic limit of the  $\text{CH}_2\text{NO}_2\text{-H}$  molecular system is located at 1.95 eV,<sup>16</sup> the lowest resonance cannot lead to a dissociative attachment, whereas the others will give rise to the emission of  $\text{CH}_2\text{NO}_2^-$  in electron attachment experiments.<sup>1</sup> The extra electron can also be weakly bound due to the high value of the dipole moment of nitromethane (3.46 D) yielding the existence of a stable dipole-bound state (DBS). Compton

*et al.*<sup>7</sup> showed that this DBS lies very close in energy to the neutral molecule ( $12 \pm 3$  meV). The two  $\sigma^*(a_1)$  resonances (denoted by  $\sigma_1^*$  and  $\sigma_2^*$ ) in nitromethane have been reported to lie at 2.4 eV, respectively, with  $\sigma_1^*$  primarily antibonding between C-N and  $\sigma_2^*$  antibonding mainly at C-H.<sup>3</sup> The expected wave functions for the DBS must be placed on the side of the molecule that contains the  $-\text{CH}_3$ , resembling therefore the orientation of the LUMO  $\pi^*_{\text{NO}}$ . However, Brooks *et al.*<sup>13</sup> have calculated the geometry of the low-lying molecular orbitals for the neutral molecule as well as in the bent geometry of the anion and shown that there is reasonably good spatial overlap between the wave function of the DBS and the lowest valence  $\sigma^*$  orbitals. This may actually result in an avoided crossing of these anionic states when plotted as a function of the C-H internuclear distance. If that is the case, the H atom may tunnel through the barrier created by the avoided crossing. Thus the coupling is most likely to occur between the  $\sigma_2^*$  and  $\pi^*_{\text{NO}}$  orbitals or through vibronic coupling between these two temporary anions as recently reported by Allan and co-workers in their work on planar unsaturated hydrocarbons substituted with halogens.<sup>21</sup> However further calculations are still needed to support these assumptions.

### 3.3 NO<sub>2</sub><sup>-</sup>

$\text{NO}_2^-$  is observed as the most intense anionic fragment. Table 2 shows the anionic states of nitromethane as determined by electron impact. As the asymptotic limit of the  $[\text{NO}_2]^- \text{-CH}_3$  molecular system is located at 0.37 eV, calculated from the bond dissociation energy and electron affinity ( $D(\text{CH}_3\text{-NO}_2) = 2.64$  eV,  $\text{EA}(\text{NO}_2) = 2.27$  eV) (Table 3), all the resonances can lead to a dissociative attachment in electron attachment experiments.<sup>1,2</sup>  $\text{NO}_2^-$  and  $\text{CH}_3\text{NO}_2^-$  ions are observed in the proportion of  $\sim 8:1$ , respectively, where this fraction is constant for all collision energies studied. This suggests that  $\text{CH}_3\text{NO}_2^-$  and  $\text{NO}_2^-$  are produced from the same resonant states.  $\text{NO}_2^-$  formation is possible due to the ionic scattering, meaning that electron transfer can occur at an early crossing of the covalent and ionic energy surfaces.

In DEA experiments,  $\text{NO}_2^-$  is formed by the accommodation of the extra (free) electron into the LUMO of  $\pi^*(b_1)$  character of the nitro group, correlating with the  ${}^2B_1$  state of  $\text{CH}_3\text{NO}_2^-$ . In the present case, the  ${}^2A_1$  state is formed by accommodation of the extra electron to the next unoccupied C-N antibonding orbital,  $\sigma^*(a_1)$ . The  $\text{K}^+$  energy loss measurements revealed a vertical electron affinity for this state of  $\sim -2$  eV (Table 2), so at thermal collision energies the effective electron affinity is expected to be much smaller, close to 0 eV.<sup>12</sup> This seems to be correlated with the DEA experiments of Sailer *et al.*<sup>2</sup> and Alizadeh *et al.*,<sup>1</sup> and the parent ion formed after the electron jump, in  $\text{K} + \text{CH}_3\text{NO}_2$  collisions, will be vibrationally excited close to the dissociation limit, correlating asymptotically with the  ${}^1A_1$  ground state of  $\text{NO}_2^-$ .

### 3.4 CNO<sup>-</sup> and CN<sup>-</sup>

Walker and Fluendy reported no negative ion formation at  $\sim 2$  eV whereas recent DEA experiments have reported production of  $\text{CNO}^-$  and  $\text{CN}^-$ .<sup>1,2</sup> However the only available

anionic state at this energy decays to the vibrationally excited neutral ground state competing with autodetachment, which may explain the low intensity signal of the present TOF mass spectrum in Fig. 1.

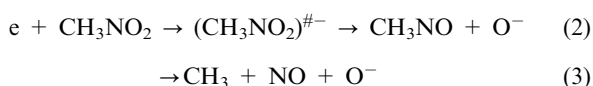
The reaction leading to  $\text{CNO}^-$  formation has been reported to be endothermic, with a signal close to 0 eV and arises only from vibrationally excited molecules.<sup>2</sup> Moreover, the third resonance listed by Sailer *et al.*<sup>2</sup> at 4.0 eV electron energy, attributed to DEA to nitromethane in the ground state, is correlated with the  $^2B_1$  state (Table 2) leading mainly to  $\text{NO}_2^-$  ( $^1B_1$ ) formation. Since the electron affinity of CNO (which, with CN, is labelled a pseudo-halogen) is higher than of  $\text{NO}_2$  (Table 3) this picture may be rationalised in terms of the available energy deposited into the metastable precursor anion and the propagation of the wave packet along the multi-dimensional potential energy surface leading to dissociation. Since  $\text{CNO}^-$  has the lowest DEA cross section ( $\sim 10^{-25} \text{ m}^2$  at 4 eV), the intensity of the fragment anion in the present experiments is also expected to be weak (Fig. 1).

### 3.5 $\text{O}^-$ and $\text{OH}^-$

Earlier time-of-flight alkali beam experiments have reported two signals attributed to  $\text{O}^-$ , mass 16 and 17 amu, one of which (17 amu) was delayed relative to the other and attributed to internal isomerisation of the  $\text{CH}_3\text{NO}_2^-$  to  $\text{CH}_3\text{ONO}^-$  prior to fragmentation.<sup>12</sup> Recently, Arenas *et al.*<sup>17</sup> have performed multiconfigurational second-order perturbation studies on the decomposition of the nitromethane radical anion and have shown no evidence of an isomerisation channel leading to the initial formation of the methylnitrite anion,  $\text{CH}_3\text{ONO}^-$ . We have therefore re-investigated masses 16 and 17 amu by deuterating nitromethane. Fig. 2a–b show negative ion TOF mass spectra of potassium with nitromethane- $\text{h}_3$  and - $\text{d}_3$  at 100 eV collision energy. The fragmentation patterns observed by deuterium substitution are shown in comparison with the - $\text{h}_3$ . There is clearly evidence of  $\text{D}^-$  (not shown here) and  $\text{OD}^-$  (Fig. 2a) formation as well as the parent anion and its dehydrogenated (deuterated) anions (Fig. 2b), allowing us to conclude that the fragment anion with mass 17 amu in  $\text{K} + \text{CH}_3\text{NO}_2$  collisions is due to  $\text{OH}^-$  formation.

$\text{O}^-$  has been reported as a major anionic product of DEA at higher incident electron energies, 5.6 and 6.1 eV,<sup>3</sup> the former producing thermal anions and the latter energetic anions with  $\sim 1$  eV translational energy. However, Walker and Fluendy were not able to distinguish whether the different  $\text{O}^-$  ions were produced from different exit channels on a single surface or from two different surfaces. They could only conclude that  $\text{O}^-$  formation results from an excited anionic state.

Dissociative electron attachment to nitromethane reported  $\text{O}^-$  formation *via* two possible reaction channels:<sup>2</sup>



where at threshold reaction (2) is operative at 2.71 eV (against a measured appearance energy of  $3.3 \pm 0.2$  eV) and reaction (3) has a calculated threshold (using  $EA(\text{O}) = 1.461$  eV,  $\Delta_f H_g^\circ(\text{CH}_3\text{NO}_2) = -81.0 \pm 0.1$  kJ mol $^{-1}$ ,  $\Delta_f H_g^\circ(\text{CH}_3) = 146 \pm 1$  kJ mol $^{-1}$ ,  $\Delta_f H_g^\circ(\text{O}) = 249.0 \pm 0.1$  kJ mol $^{-1}$ , Table 3)

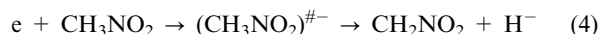
at 4.41 eV.<sup>2</sup> However, due to the shape of the DEA cross section, a slow increase as a function of the electron energy, Sailer *et al.*<sup>3</sup> concluded that  $\text{O}^-$  formation through reaction (3) does not occur at the thermodynamical threshold and the estimated values are upper limits. The more recent DEA experiments of Alizadeh *et al.*,<sup>1</sup> reported a strong  $\text{O}^-$  signal at 6 eV and at the other high energy resonances at 9 and 10.5 eV, which has been explained in terms of core-excited resonances and/or Rydberg excitation, respectively. Therefore, the  $\text{K}^+$  energy loss profiles of ref. 12 show above 61 eV collision energy broad features at  $\sim 6.5$  and 8.5 eV and extending up to  $\sim 13$  eV for higher collision energies (183 eV). This may be indicative of the resonant character of the accessible channel leading to  $\text{O}^-$ .

$\text{OH}^-$  formation is shown at a resonant electron energy of  $\sim 4.0$  eV and was explained by electron capture which distorts the molecular anion about the HCNO dihedral angle narrowing the OH distance.<sup>3</sup> A tentative assignment was proposed for the initial population of  $^2B_1$  state as the precursor. However, Sailer *et al.*<sup>2</sup> have shown that  $\text{OH}^-$  formation also occurs *via* two low electron energy resonances at  $\sim 0$  and 1.7 eV. They have argued, based on the gas pressure in the reaction chamber and absence of contaminants, that the lowest resonance ( $\sim 0$  eV) is due to DEA to vibrationally excited (hot bands) nitromethane molecules. In fact, in the three mechanisms proposed for  $\text{OH}^-$  formation, two of them involve considerable rearrangement of the bonds and are endothermic by  $\sim 1$  eV.

### 3.6 $\text{H}^-$

The spectra in Fig. 1 show the recorded  $\text{H}^-$  signal obtained by subtracting the background signal (with a pressure of  $4 \times 10^{-5}$  Pa) from the sample signal (at a working pressure of  $10^{-4}$  Pa). However, it is worth noting that  $\text{D}^-$  yield at 100 eV collision energy (not shown here) is around half that of  $\text{H}^-$ .

The DEA reaction leading to  $\text{H}^-$  formation has been identified as:<sup>1</sup>



which is complementary to (1), with a threshold at 3.65 eV ( $D(\text{CH}_2\text{NO}_2\text{-H}) = 4.40$  eV and the electron affinity  $EA(\text{H}) = 0.75$  eV (Table 3)), below the reported experimental threshold at  $\sim 4.5$  eV.<sup>1</sup> DEA to nitromethane producing  $\text{H}^-$  shows two broad resonant structures peaking at 7.5 and 9.0 eV which have been identified as signatures of core-excited resonances initiated *via* ( $\sigma \rightarrow \pi^*$ ) or ( $\pi \rightarrow \pi^*$ ) electronic transitions.<sup>1,3</sup> This seems to be consistent with the energy loss spectra of  $\text{K}^+$  ions formed in the forward direction at several collision energies.<sup>12</sup> Although these earlier TOF mass experiments were not able to detect  $\text{H}^-$ , the energy loss profiles, especially above 61 eV collision energy, show a broad structure peaking at 8 eV and extending to  $\sim 13$  eV, which is particularly visible in the 183 eV incident  $\text{K}^\circ$  beam profile.

It should be noted that the  $\text{H}^-$  TOF mass spectrum at 100 eV shows some structure on the peak's right side amounting around one third of its height (Fig. 1). This contribution is an artefact from the potassium hyperthermal neutral atoms ( $\text{K}^\circ$ ) pulsed signal. The extraction pulse has to be sufficiently wide

to allow for the heavier fragments to be fully extracted, which in turn means that for the lighter fragments, as is the case of the  $\text{H}^-$ , an enhancement in the rate of creation is observed while the ( $\text{K}^\circ$ ) pulsed signal lasts in the interaction region. The width of the shoulder can be adjusted in order to not interfere with the neighbouring anions, which can be particularly useful to detect  $\text{D}^-$ .

## 5. Conclusions

The present electron transfer studies to nitromethane constitute a more extensive study than earlier work employing a higher mass resolution time-of-flight mass spectrometer than before. In addition to the three anions observed in previous studies, production of  $\text{CH}_3\text{NO}_2^-$ ,  $\text{CH}_2\text{NO}_2^-$ ,  $\text{CNO}^-$ ,  $\text{NO}^-$ ,  $\text{CN}^-$ ,  $\text{OH}^-$ , and  $\text{H}^-$  has been observed.

Although rather complex the dynamics after electron transfer by nitromethane seems to be non-statistical which was also reported in the spectroscopy and dynamics studies of negative ions of Walker and Fluendy.<sup>3</sup> The formation of  $\text{CH}_2\text{NO}_2^-$ ,  $\text{NO}_2^-$ ,  $\text{CNO}^-$ ,  $\text{CN}^-$  and  $\text{OH}^-$ , through low energy resonances may be explained in terms of dissociative electron attachment to highly vibrationally excited molecules—hot bands. In atom-molecule collisions, the  $\text{K}^+$  ion can strongly interact with the transient molecular anion, and if bond stretching is allowed in the target molecule during the electron transfer, strong vibronic coupling may occur. TOF mass spectra in Fig. 1 show the ionic yields dependence as a function of the collision energy. The lowest laboratory collision energy, 30 eV ( $\sim 18$  eV in the centre of mass), is still above the threshold for electron transfer (3.9 eV), and therefore the negative molecular ion can be formed with an excess of internal energy which even might result in fragmentation dictating the nature of the negative fragment ions formed.

## Acknowledgements

We wish to acknowledge Prof. Luísa Ferreira from the Department of Chemistry, Universidade Nova de Lisboa, for purifying the nitromethane ( $-\text{h}_3$ ) compound. R. A. and D. A. acknowledge the Portuguese Foundation for Science and Technology (FCT-MCTES) for post-graduate scholarships SFRH/BD/32271/2006 and SFRH/BD/61645/2009, respectively. P. L. V. acknowledges the visiting research fellow position in the Department of Physics and Astronomy, The Open University,

UK, and together with N. J. M. the support from the British Council for the Portuguese–English joint collaboration and together with G. G. from CSIC, Madrid for the Spanish-Portuguese Project HP2006-0042; Ministerio de Ciencia e Innovación (project FIS2009-10245). Some of this work forms part of the EU/ESF COST Actions Electron Controlled Chemical Lithography (ECCL) CM0601 and The Chemical Cosmos Action CM0805.

## References

- 1 E. Alizadeh, F. Ferreira da Silva, F. Zappa, A. Mauracher, M. Probst, S. Denifl, A. Bacher, T. D. Märk, P. Limão-Vieira and P. Scheier, *Int. J. Mass Spectrom.*, 2008, **271**, 15.
- 2 W. Sailer, A. Pelc, S. Matejčík, E. Illenberger, P. Scheier and T. D. Märk, *J. Chem. Phys.*, 2002, **117**, 7989.
- 3 I. C. Walker and M. A. D. Fluendy, *Int. J. Mass Spectrom.*, 2001, **205**, 171.
- 4 A. Modeli and M. Venuti, *Int. J. Mass Spectrom.*, 2001, **205**, 7.
- 5 R. N. Compton, P. W. Reinhardt and C. D. Cooper, *J. Chem. Phys.*, 1978, **68**, 4360.
- 6 J. A. Stockdale, F. J. Davis, R. N. Compton and C. E. Klots, *J. Chem. Phys.*, 1974, **60**, 4279.
- 7 R. N. Compton, H. S. Carman Jr, C. Desfrancois, H. Abdoul-Carime, J. P. Schermann, J. H. Hendricks, S. A. Lyapustina and K. H. Bowen, *J. Chem. Phys.*, 1996, **105**, 3472.
- 8 F. Lecomte, S. Carles, C. Desfrancois and M. A. Johnson, *J. Chem. Phys.*, 2000, **113**, 10973.
- 9 L. Suess, R. Parthasarathy and F. B. Dunning, *J. Chem. Phys.*, 2003, **119**, 9532.
- 10 Y. Liu, M. Cannon, L. Suess, F. B. Dunning, V. E. Chernov and B. A. Zon, *Chem. Phys. Lett.*, 2006, **433**, 1.
- 11 D. J. Goebbert, K. Pichugin and A. Sanov, *J. Chem. Phys.*, 2009, **131**, 164308.
- 12 R. F. M. Lobo, A. M. C. Moutinho, K. Lacmann and J. Los, *J. Chem. Phys.*, 1991, **95**, 166.
- 13 P. R. Brooks, P. W. Harland and C. E. Redden, *J. Phys. Chem. A*, 2006, **110**, 4697; P. R. Brooks, P. W. Harland and C. E. Redden, *J. Am. Chem. Soc.*, 2006, **128**, 4773.
- 14 L. Adamowicz, *J. Chem. Phys.*, 1989, **91**, 7787.
- 15 T. Sommerfeld, *Phys. Chem. Chem. Phys.*, 2002, **4**, 2511; T. Sommerfeld, *J. Phys. Conf. Ser.*, 2005, **4**, 245.
- 16 G. L. Gustev and R. J. Bartlett, *J. Chem. Phys.*, 1996, **105**, 8785.
- 17 J. F. Arenas, J. C. Otero, D. Peláez, J. Soto and L. Serrano-Andrés, *J. Chem. Phys.*, 2004, **121**, 4127.
- 18 P. Limão-Vieira, private communication.
- 19 A. Di Domenico and J. L. Franklin, *Int. J. Mass Spectrom. Ion Phys.*, 1972, **9**, 171.
- 20 I. Hahndorf, E. Illenberger, L. Lehr and J. Manz, *Chem. Phys. Lett.*, 1994, **231**, 460.
- 21 T. Skalicky, C. Chollet, N. Pasquier and M. Allan, *Phys. Chem. Chem. Phys.*, 2002, **4**, 3583.